Efficient Tissue Ablation using a Laser Tunable in the Water Absorption Band at 3 microns with little collateral damage

Alexandra Nierlich[1], Danail Chuchumishev[1,2], Elizabeth Nagel[1], Kristiana Marinova[2], Stanislav Philipov[3], Torsten Fiebig[1], Ivan Buchvarov[1,2], Claus-Peter Richter[1,4,5]
[1]Deptartment of Otolaryngology, Northwestern University, 303 E. Chicago Ave, Searle 12-561, Chicago, IL 60611, USA, [2]Department of Physics, Sofia University, 5 James Bourchier Blvd., Sofia, 1164, Bulgaria; [3]Department of Medicine, Sofia University, 1 Kozyak Str., Sofia, Bulgaria; [4]Department of Biomedical Engineering, Northwestern University, 2145 Sheridan Road, Tech E310, Evanston, IL 60208, USA; [5]The Hugh Knowles Center, Department of Communication Sciences and Disorders, Northwestern University, Evanston, IL 60208, USA

ABSTRACT

Lasers can significantly advance medical diagnostics and treatment. At high power, they are typically used as cutting tools during surgery. For lasers that are used as knifes, radiation wavelengths in the far ultraviolet and in the near infrared spectral regions are favored because tissue has high contents of collagen and water. Collagen has an absorption peak around 190 nm, while water is in the near infrared around 3,000 nm. Changing the wavelength across the absorption peak will result in significant differences in laser tissue interactions. Tunable lasers in the infrared that could optimize the laser tissue interaction for ablation and/or coagulation are not available until now besides the Free Electron Laser (FEL). Here we demonstrate efficient tissue ablation using a table-top mid-IR laser tunable between 3,000 to 3,500 nm. A detailed study of the ablation has been conducted in different tissues. Little collateral thermal damage has been found at a distance above 10-20 microns from the ablated surface. Furthermore, little mechanical damage could be seen in conventional histology and by examination of birefringent activity of the samples using a pair of cross polarizing filters.

Keywords: laser-tissue interaction, near-infrared, laser, ablation, surgery

1. INTRODUCTION

Over the last decades the introduction of lasers has advanced several medical disciplines and opened completely novel treatment opportunities in medical areas such as neurosurgery, cardiology, dentistry, urology, or dermatology [1-4]. The procedures and the methods for medical treatment and research take advantage of a wide variety of laser-tissue interaction mechanisms, including photothermal, photomechanical and photochemical interactions [4, 5]. Recently, there has been increasing interest in the use of lasers in the infrared (IR) region. For this range the penetration depth of the radiation changes drastically [6]. Changing the wavelengths of the laser would allow one to fine tune laser tissue interactions (penetration depth and radiant energy density), minimizing the collateral heating effects in a tissue specific manner. Moreover, the latest solid-state laser technology ensures small and compact design and fiber optic delivery options. Hence, these lasers are indispensable for minimally invasive surgery. Currently, there are several commercial IR lasers available that have individual (fixed) single wavelength output and thus, their application range is strongly limited to specific surgical tasks performed at those specific wavelengths. In other words, some lasers are ideal for tissue cutting in fluid-filled spaces, while others for kidney stone fragmentation or coagulation of the tissue etc. [4]. Instead of using multiple separate laser units – which is practically impossible – it would be economically and practically efficient to combine the many characteristic features each laser system provides into a *single compact table-top laser instrument*. Here we present the results obtained with such a novel laser.

*cri529@northwestern.edu; phone 1 312 503 1603; fax 1 312 503 1616

Photonic Therapeutics and Diagnostics X, edited by Bernard Choi, et al., Proc. of SPIE
Vol. 8926, 89262H · © 2014 SPIE · CCC code: 1605-7422/14/$18 · doi: 10.1117/12.2049339

2. MATERIALS AND METHODS

2.1 The laser

In order to generate coherent radiation with high average power and high pulse energy in the spectral region between 3,000 and 3,500 nm, a nonlinear frequency down-conversion stage was constructed and pumped by Nd-based master oscillator power amplifier (MOPA). The MOPA design was similar to the one described in [7]. It consisted of a microchip laser which pulses were amplified by two diode-pumped Nd:YAG boost amplifiers, operated in a double pass regime, thus providing 35 mJ pulses with high beam quality ($M_x^2 \times M_y^2$=1.3 × 1.1) and short pulse duration (1.4 ns), at 0.5 kHz repetition rate. The frequency down-conversion stage employed a sub-nanosecond, short cavity, singly-resonant optical parametric oscillator (OPO), based on a large aperture periodically poled stoichiometric lithium tantalate (PPSLT) [8]. A 20 mm long, 10 mm wide, and 3.2 mm (along z axis) thick PPSLT crystal was used with three poled zones with different domain inversion periods (30.2, 30.3 and 30.4 μm) and the generated output idler energy was 0.48 mJ at 3,100 nm wavelength, when pumped with 3.48 mJ, corresponding to an idler conversion efficiency of 13.8 %. In order to further increase the idler energy an optical parametric amplifier (OPA) was added, which employed a similar 37 mm long PPSLT crystal. When pumped with 30 mJ the maximum achieved output idler energy from the OPA was 5.7 mJ with pulse duration ~1.4 ns at 0.5 kHz repetition rate, corresponding to idler conversion efficiency of 19 % and a total conversion efficiency of 51 %. By changing the temperature of the two PPSLT crystals from 40°C up to 265 °C and employing the three domain inversion periods, continuous tunability of the laser from 3,000 to 3,500 nm was achieved.

2.2 Experimental design

Mounting and irradiation of the tissue: Fixed cadaveric tissue was used to test the laser instrument. The tissue samples have been taken from pigs and include skin, cartilage, and bone. Small samples (2x2x3 mm^3) were prepared and mounted to a 2D motorized holder. During irradiation the sample surface was at the focal point of the laser beam. The tissue was either exposed to ten single pulses delivered to the same tissue site or to a train of pulses. During the tissue exposure to the train of pulses, the specimen was advanced with 0.1 to 2 mm/s. The repetition rate of the laser pulses was 500 Hz. The radiant energy per pulse was 3.0, 2.9, and 2.3 mJ at 3,000, 3,320, and 3,470 nm radiation wavelength, respectively. The pulse length was ~1.4 ns. The laser spot had an oval shape with a long axis of 350 μm and a short axis of 250 μm. The beam profile was Gaussian.

Histology: Following the irradiation of the tissue, the specimens were kept in saline solution. Following standard histological protocols, the specimen were decalcified if necessary, dehydrated, and embedded. The embedded specimens were serial sectioned at 5 μm, mounted on glass slides, and stained with hematoxylin and eosin or Luna. Bright field images of selected sections were examined with a light microscope (Leica DMRB, Buffalo Grove, IL) after they were captured with a Spot Insight Color camera (SPOT™ Imaging Solutions, Sterling Heights, MI). Images were analyzed for tissue carbonization or loss of birefringent activity when examined under a pair of cross-polarizing filters [9].

Data analysis: Sections were visually examined with a Zeiss Axio Imager.A1 Light Microscope (Carl Zeiss, Göttingen, Germany). Images were captured and stored on a PC. Using ImageJ the width, the depth, and the cross sectional area of the ablation crater was determined after the program was calibrated (Fig. 1). Data were plotted for different wavelengths and results were compared. Images captured with cross-polarizing filters were used to determine birefringent activity. From the loss of the birefringent activity the thermal damage zone of the laser ablation was estimated (Fig. 2).

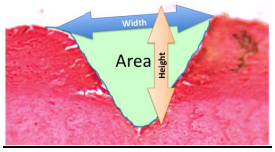

Figure 1. The image shows the ablation crater in cartilage tissue from a pigs ear. For analysis the width (blue arrow), the depth (orange arrow and the area (green) has been determined. Measures were obtained with ImageJ.

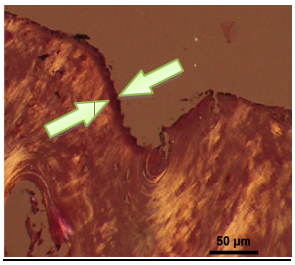

Figure 2. The image was captured using cross-polarizing filters and shows the ablation crater in the bone. Birefringent activity can be seen. To estimate the thermal damage the width of loss in birefringent activity was used (zone between the arrows). Linear measures were obtained with ImageJ.

3. RESULTS

The laser device was tested for its ability to ablate tissue and for its corresponding tissue damage. The selected laser parameters for the novel instrument were sufficient for tissue ablation. Tissue ablations were seen for skin at every tested wavelength, but not for the cartilage. Results are presented in the text and summarized in Table 1. At 3,060 nm, skin ablation craters had an average depth of 113 µm. When the same skin tissue was irradiated at a wavelength of 3,320 nm, the ablation crater was on average 178 µm. At 3,490 nm the averaged depth for the ablation was 178 µm (Fig. 3). This was different for cartilage. The ablations crater was smaller than for skin tissue. On average, the depth decreased from 96 to 78 µm and no ablation as the wavelength increased from 3,060 nm to 3,490 nm (Fig. 3 and 4, Table 1).

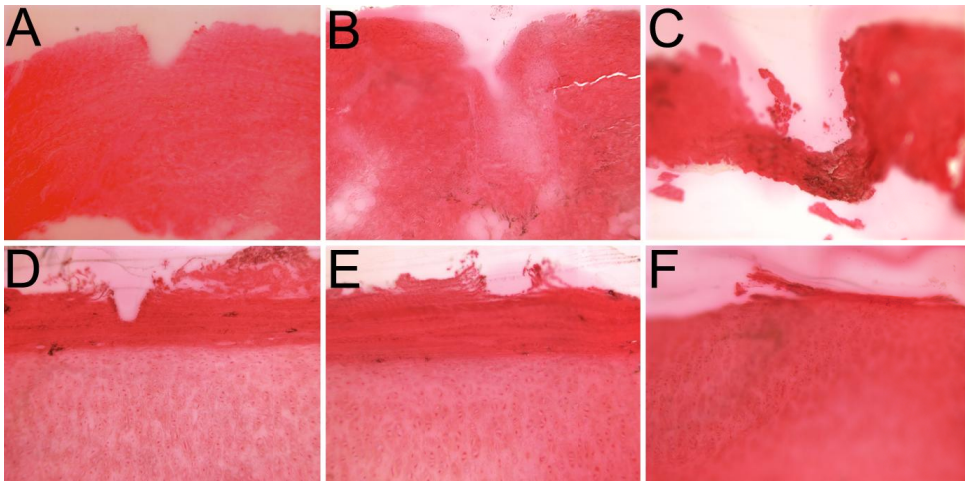

Figure 3. Images obtained after tissue ablation with 10 single laser pulses delivered at one selected site. Top row shows pig-skin and bottom row cartilage from the pig pinna. Radiation wavelength was 3,060 nm for A and D, 3,320 nm for B and E, and 3,490 nm for C and F. While the ablation crater increased for skin with increasing wavelength, the crater decreased for cartilage. At 3,060 nm little difference in ablation was seen.

Pig								
3,060 nm			3,320 nm			3,490 nm		
cartilage								
width (µm)	depth (µm)	area (mm^2)	width (µm)	depth (µm)	area (mm^2)	width (µm)	depth (µm)	area (mm^2)
127±27 N=4	96±9 N=4	0.009±0.003 N=4	115±15 N=3	78±15 N=3	0.007±0.002 N=3	n.d.	n.d.	n.d.
skin								
width (µm)	depth (µm)	area (mm^2)	width (µm)	depth (µm)	area (mm^2)	width (µm)	depth (µm)	area (mm^2)
162±39 N=3	113±18 N=3	0.014±0.001 N=3	163±44 N=2	178±17 N=2	0.019±0.016 N=2	275±99 N=2	178±17 N=2	0.076±0.031 N=2

Table 1: Table 1 summarizes the data obtained for two tissue types obtained from the pig at different radiation wavelengths. Data are plotted as well in Figure 4.

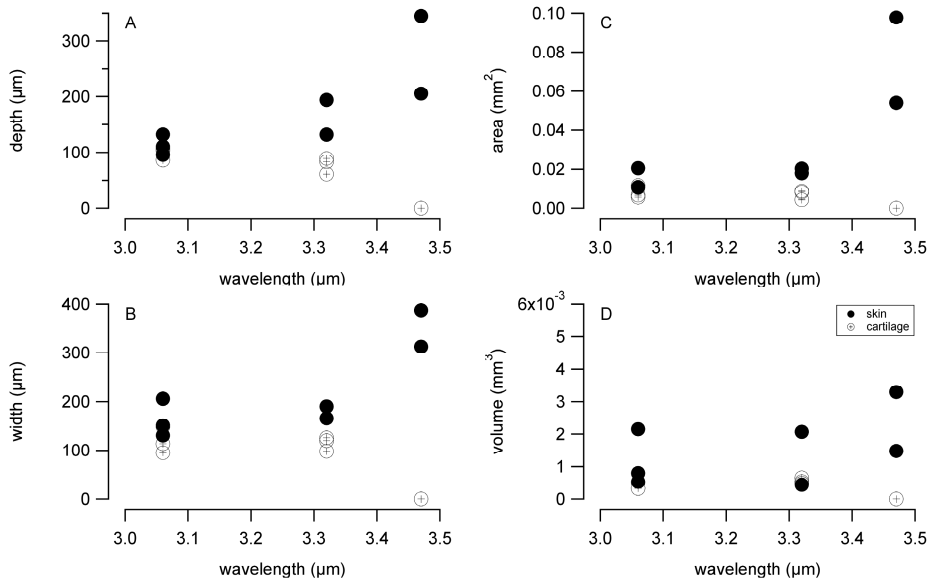

Figure 4. Shown are the dimensions for the ablation crater. The **left top** panel shows the depth, which increases for skin with increasing wavelength but decreases for cartilage. No ablation could be seen at 3,490 nm for cartilage. The **left bottom** panel shows the width of the ablation crater, which increases for skin with increasing wavelength but decreases for cartilage. No ablation could be seen at 3,490 nm for cartilage. The **right top** panel shows the cross sectional area of the ablation crater. It increases for skin with increasing wavelength but decreases for cartilage. No ablation could be seen at 3,490 nm for cartilage. The **right bottom** panel shows sum of all cross-sectional areas obtained from serial sections of the samples. The volume, which increases fop skin with increasing wavelength but decreases for cartilage. No ablation could be seen at 3,490 nm for cartilage.

Collateral damage from the irradiation with the laser was determined by examining images that were captured with brightfield and with cross-polarizing filters. The images shown in Figure 4 are the same samples shown in Figure 3 but were captured with cross-polarizing filters. No carbonization was seen and the loss in birefringent activity was less than 20 µm (Fig. 4). No other signs for thermal or mechanical damage such as tissue dessication, water vapor vacuole formation and explosive fragmentation could be detected. One should note that the current examination and judgment is based on fixed cadaveric material, and has been examined with light microscopy only.

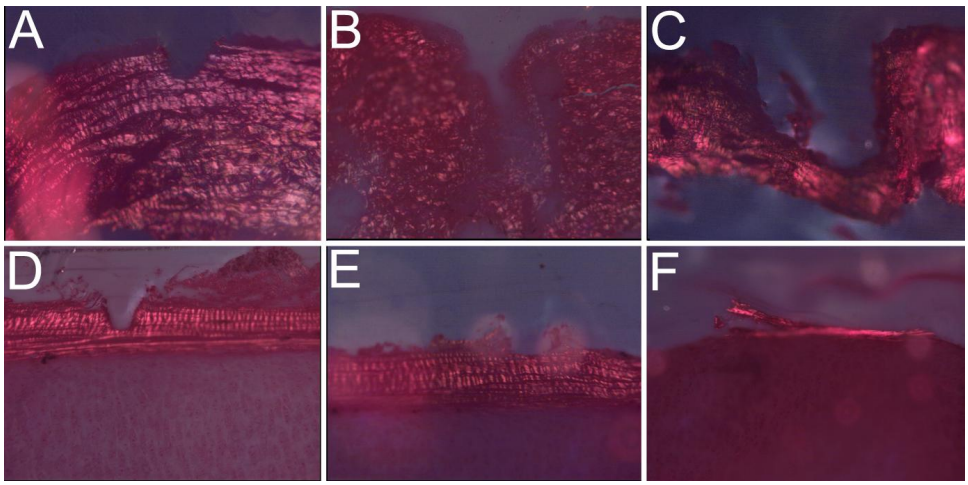

Figure 5. Images obtained after tissue ablation with 10 single laser pulses delivered at one selected site. The samples are the same shown in Figure 3 and were captured with cross-polarized filters. The top row shows pig-skin and bottom row cartilage from the pig pinna. Radiation wavelength was 3,060 nm for A and D, 3,320 nm for B and E, and 3,490 nm for C and F. The loss in birefringent activity was almost not detectable, in some view cases less than 50 µm. No correlation of amount of tissue damage and with radiation wavelength could be established.

The bone sample held slightly different results. With increasing of the number of pulses delivered, the depth of the groove increased (data not shown). Along the ablation grove a thin black line can be seen in the left brightfield image, indicating the carbonization of the organic tissue (Fig. 6, left panel). Next to the carbonization line, a small tissue layer, about 10-20 µm thick, shows a small layer of darker staining (Fig. 6, left panel). This is the layer, for which thermal damage could be detected. The damage could be verified by the loss of optical activity as judged from the birefringence seen under cross-polarizing imaging conditions (Fig 6, right panel).

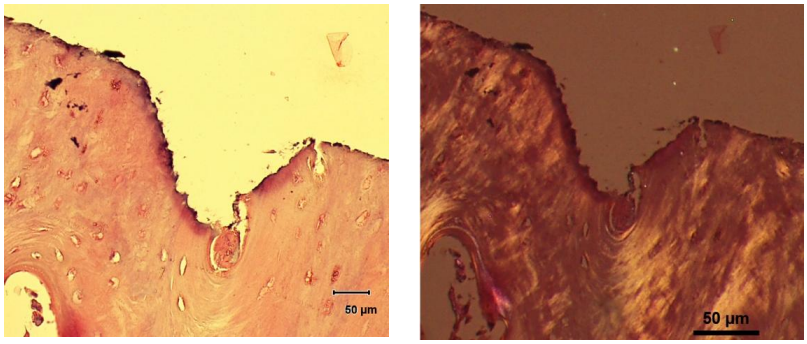

Figure 6. Histological sections of irradiated bones from pigs. In the left panel a bright field images is presented. The dark line along the ablation groove shows the black lining resulting form the carbonization of the organic tissue. Beyond the carbonization a thin (~10 µm) wide line that revealed heat damage can be seen (see arrows). Imaging of the tissue with a pair of cross polarizing filters (right panel) confirms the findings seen in the hematoxylin-eosin staining in the left panel. Only a thin layer of about 10-20 µm losses its birefringent activity after the tissue ablation.

4. DISCUSSION

A tunable laser in the near infrared has been built and tested that is powerful enough to ablate soft tissue and bone. At penetration depths of the radiation less than 10 µm, the ablation was possible with little collateral thermal damage. Our initial evaluations of the exposed tissue sections and images with cross-polarizing filters confirmed the finding that ablation is possible with minimal collateral damage to the tissue.

Light microscopy was used to evaluate damages resulting from irradiating the tissue. With this method subtle changes will not be detected. Survival experiments are required to allow for damages to develop. On the other hand, thermal damages that often occur are minimal with the novel laser instrument. This is true for single pulses and for laser pulses presented at fast repetition rates, here 500 Hz. *In vivo* experiments are necessary to determine longterm damages that cannot be seen with light microscopy or that require days or week to develop.

The ablation crater did not change drastically in size with changing wavelength. Moreover, the ablation crater was similar among the tissue types at 3,060 nm radiation wavelength. Differences among the tissues were observed for wavelengths with longer penetration depths of the photons into the tissue. In general tissues with an organized collagen structure tended to show smaller ablation than loosely connected tissues.

A limitation of this study is the use of fixed cadaveric tissue. Since the hydration of the tissue is different in vivo and the main absorber at the selected wavelength is water, ablation may depend on the hydration of the tissue. Control experiments are on the way to establish the changes that occur after euthanizing the animal. Furthermore, experiments are on the way to determine whether the novel laser instrument can be used in close proximity to nerve or other neural structures.

5. ACKNOWLEDGEMENTS

This work was funded by a grant from the NIH, 8R21EB015899 and in part by the Bulgarian National Science Fund under grants number DDVU 02/105/2010.

REFERENCES

[1] Niemz, M.H. and SpringerLink (Online service), *Laser-tissue interactions fundamentals and applications*, in *Biological and medical physics, biomedical engineering*2007, Springer: Berlin.

[2] Welch, A.J. and M.J.C. van Gemert, *Optical-Thermal Response of Laser-Irradiated Tissue.* second ed2012, New York: Plenum Press.

[3] Tuchin, V., *Tissue optics : light scattering methods and instruments for medical diagnosis*. Tutorial texts series2000, Bellingham, Wash.: SPIE Press. xxv, 352 p.
[4] Vogel, A. and V. Venugopalan, *Mechanisms of pulsed laser ablation of biological tissues.* Chemical reviews, 2003. **103**(2): p. 577-644.
[5] Jacques, S.L., *Laser-tissue interactions. Photochemical, photothermal, and photomechanical.* Surg Clin North Am, 1992. **72**(3): p. 531-58.
[6] Hale, G.M. and M.R. Querry, *Optical constants of water in the 200 nm to 200 μm region.* Appl Opt, 1973. **12**: p. 555-563.
[7] Chuchumishev, D., et al. *Near Diffraction Limited Pulses with 52-mJ, 1.2 ns at 0.5 kHz, Generated by Nd-based MOPA*. in *CLEO/Europe and IQEC 2013 Conference Digest*. 2013. Munich: Optical Society of America.
[8] Chuchumishev, D., et al., *Subnanosecond, mid-IR, 0.5 kHz periodically poled stoichiometric LiTaO3 optical parametric oscillator with over 1 W average power.* Optics Letters, 2013. **38**(17): p. 3347-3349.
[9] Pearce, J. and S. Thomsen, *Rate process analysis of thermal damage.*, in *Optical-thermal response of laser irrdiated tissue.*, A.J. Welch and M.J.C. van Gemert, Editors. 1995, Plenum Press: New York and London. p. 561-606.